Inelastic Neutron Scattering Study of Electron Reduction in Mn 12 Derivatives

ARTICLE *in* INORGANIC CHEMISTRY · MARCH 2005

Impact Factor: 4.76 · DOI: 10.1021/ic048931p · Source: PubMed

9 AUTHORS, INCLUDING:

Monica Soler
University of Chile
36 PUBLICATIONS **1,396** CITATIONS
SEE PROFILE

George Christou
University of Florida
758 PUBLICATIONS **29,434** CITATIONS
SEE PROFILE

Ruep Ekkehard Lechner
European Spallation Source
169 PUBLICATIONS **2,528** CITATIONS
SEE PROFILE

Inorg. Chem. **2005**, *44*, 649–653

Inelastic Neutron Scattering Study of Electron Reduction in Mn_{12} Derivatives

Reto Basler, Andreas Sieber, Grégory Chaboussant,* and Hans U. GUdel

Department of Chemistry and Biochemistry, University of Berne, Freiestrasse 3, CH-3000 Berne 9, Switzerland

Nicole E. Chakov, Monica Soler, and George Christou

Department of Chemistry, University of Florida, Gainesville, Florida 32611-7200

Arnaud Desmedt† and Ruep Lechner

Hahn-Meitner Institut, D-14109 Berlin-Wannsee, Germany

Received August 5, 2004

We report inelastic neutron scattering (INS) studies on a series of Mn_{12} derivatives, $[Mn_{12}O_{12}(O_2CC_6F_5)_{16}(H_2O)_4]^z$, in which the number of unpaired electrons in the cluster is varied. We investigated three oxidation levels: $z = 0$ for the neutral complex, $z = -1$ for the one-electron reduced species and $z = -2$ for the two-electron reduced complex. For $z = 0$, the ground state is $S = 10$ as in the prototypical Mn_{12}-acetate. For $z = -1$, we have $S = {}^{19}/_2$, and for $z = -2$, an $S = 10$ ground state is retrieved. INS studies show that the axial zero-field splitting parameter D is strongly suppressed upon successive electron reduction: $D = -0.45$ cm^{-1} ($z = 0$), $D = -0.35$ cm^{-1} ($z = -1$), and $D \approx -0.26$ cm^{-1} ($z = -2$). Each electron reduction step is directly correlated to the conversion of one anisotropic (Jahn–Teller distorted) Mn^{3+} ($S = 2$) to one nearly isotropic Mn^{2+} ($S = {}^5/_2$).

I. Introduction

The notion of single-molecule magnets (SMMs) was coined to describe a macroscopic assembly of identical and isolated molecules with superparamagnetic behavior. Each single magnetic molecule (spin cluster) shows magnetization hysteresis and very slow magnetization relaxation at low temperatures.[1,2] SMMs are therefore potential candidates to develop information storage and computing devices at the molecular level.[3,4] There are several important parameters that control the low temperature properties. Each cluster should have a large spin ground state S and a large negative axial anisotropy $D < 0$ and must be magnetically isolated from its neighbors. A consequence of these combined properties is that each molecule possesses an energy barrier ($U \approx -DS^2$) to magnetization reversal. At low temperatures, the magnetization is blocked, hysteresis loops are observed, and the relaxation occurs only by tunneling channels through the anisotropy barrier.[5]

The mixed-valence (Mn^{3+}/Mn^{4+}) compound Mn_{12}−acetate ($S = 10$, $D = -0.47$ cm^{-1}) is the best studied SMM, and numerous experiments have demonstrated its ability to show remarkable fingerprints of SMM behavior.[6,3] However, despite intense efforts to synthesize new, improved magnetic clusters,[7−12] it still has the highest energy barrier to date. Mn_{12}−acetate is a crystalline material consisting of magnetic molecules where the magnetically active ions are arranged

* To whom correspondence should be addressed. Present address: Laboratoire Léon Brillouin, CEA Saclay, 91191 Gif-sur-Yvette Cedex, France. E-mail: chabouss@llb.saclay.cea.fr.

† Present address: LPCM-CNRS, University of Bordeaux, F-33405 Talence Cedex, France.

(1) Sessoli, R.; Tsai, H.-L.; Schake, A. R.; Wang, S.; Vincent, J. B.; Folting, K.; Gatteschi, D.; Christou, G.; Hendrickson, D. N. *J. Am. Chem. Soc.* **1993**, *115*, 1804.

(2) Sessoli, R.; Gatteschi, D.; Caneschi, A.; Novak, M. A. *Nature* **1993**, *356*, 141.

(3) For a recent review: Sessoli, R.; Gatteschi, D. *Angew. Chem., Int. Ed.* **2003**, *42*, 268.

(4) Leuenberger, M. N.; Loss, D. *Nature* **2001**, *410*, 789.

(5) Barbara, B.; Thomas, L.; Lionti, F.; Chiorescu, I.; Sulpice, A. *J. Magn. Magn. Mater.* **1999**, *200*, 167.

(6) Thomas, L.; Lionti, F.; Ballou, R.; Gatteschi, D.; Sessoli, R.; Barbara, B. *Nature* **1996**, *383*, 145.

(7) Aubin, S. M. J.; Sun, Z.; Hendrickson, D. N.; Guzei, I. A.; Arnold, A. L.; Christou, G. *Chem. Commun.* **1997**, *22*, 2239.

10.1021/ic048931p CCC: $30.25
Published on Web 01/11/2005

into two groups: A central core made up of a tetrahedron of 4 Mn^{4+} ($S = {}^3/_2$) and an external ring of 8 Mn^{3+} ($S = 2$) ions. Neighboring Mn ions are coupled in an intricate pattern via different types of μ-oxo bridges by which both AFM and FM exchange couplings can be present in this system. The magnetic ground state has a total spin $S = 10$. This is rationalized by a ferrimagnetic-type arrangement, i.e., the 8 Mn^{3+} pointing "up" and the 4 Mn^{4+} pointing "down". Moreover, each Mn_{12} cluster is only weakly coupled to its neighbors such that there is no long-range magnetic ordering down to the millikelvin range.

In this context, to obtain a larger spin ground state S and/or a more negative anisotropy D it is crucial to better understand the effects of chemical and physical variations on these parameters. Consequently, we have undertaken an inelastic neutron scattering (INS) study of three-electron reduced Mn_{12} complexes. In such systems, INS is a powerful tool to obtain detailed magnetic information like magnetic anisotropy parameters (axial, rhombic, and up to the fourth order) as it does not rely on applying a magnetic field. The compounds are the pentafluorobenzoate Mn_{12} complexes $[Mn_{12}O_{12}(O_2CC_6F_5)_{16}(H_2O)_4]^z$. The electron reduction degree z can be 0, -1, or -2 without major change in the structure.[13,14] Previous experiments on Mn_{12}−acetate[16,15] and other molecular magnets[11,18−21] have shown that one can derive the anisotropy parameters with great accuracy.

II. Experimental Section

A. Samples. In the following, $[Mn_{12}O_{12}(O_2CC_6F_5)_{16}(H_2O)_4]$ is noted sample **1**, the one-electron reduced $[Mn_{12}O_{12}(O_2CC_6F_5)_{16}(H_2O)_4]^{1-}$ is noted sample **2**, and the two-electron reduced $[Mn_{12}O_{12}(O_2CC_6F_5)_{16}(H_2O)_4]^{2-}$ is noted sample **3**. Structural details are given in ref 13. The structure of **1** is similar to previously characterized neutral Mn_{12} complexes. The $Mn_{12}O_{12}$ block is virtually identical to Mn_{12}−acetate, and peripheral ligation is achieved by 16 bridging $F_5C_6CO_2^-$ ligands and 4 terminal H_2O groups. The Mn^{3+} ions are octahedrally coordinated and show an axial Jahn−Teller (JT) elongated axis approximately pointing parallel to S_4, i.e., the easy axis of the molecule. For samples **2** and **3**, the overall structure is preserved, but analysis of the Mn−O bond lengths shows that while the central tetrahedron of Mn^{4+} ions is unaffected, the outer Mn^{3+} are successively reduced to Mn^{2+} ions upon addition of one and two electrons, respectively.[13]

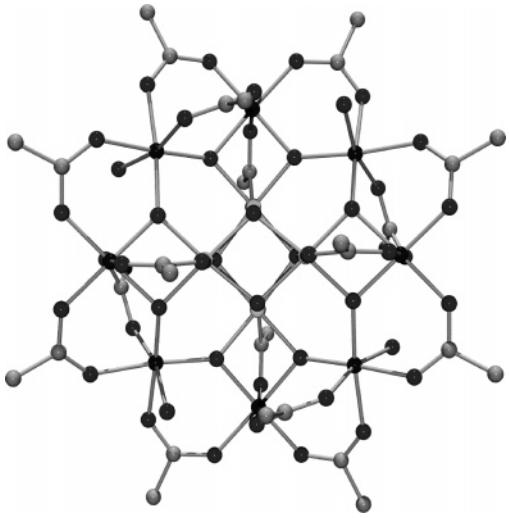

Figure 1. View of the molecular complex $[Mn_{12}O_{12}(O_2CC_6F_5)_{16}(H_2O)_4]^z$ with $z = 0$.[13]

Magnetic measurements show that the three compounds retain the SMM properties of the original complex, Mn_{12}−acetate. The ground states are shown to vary upon electron reduction: $S = 10$ for $z = 0$ and $z = -2$, and $S = {}^{19}/_2$ for $z = -1$.[13] The effective energy barrier shows a clear decrease upon successive electron reduction.

B. Inelastic Neutron Scattering. The polycrystalline powder samples were placed under helium into a rectangular flat aluminum container of dimensions 43 × 61 × 5 mm^3, with an accessible sample volume of 30 × 50 × 3 mm^3 for **1** and **3** and 30 × 50 × 2 mm^3 for **2**. INS experiments were performed on the time-of-flight spectrometer NEAT at the Hahn-Meitner Institute (HMI) in Berlin, using cold neutrons of wavelength $\lambda = 6.0$ Å. This resulted in a resolution of about 70 μeV (fwhm) at the elastic line. Data were collected at several temperatures between 1.8 and 20 K and were corrected for the detector efficiency by means of the spectrum of vanadium metal. Data reduction was performed using the program INX. The background of each spectrum was estimated from a polynomial fit to the baseline of the low temperature spectra for each compound and then subtracted. The analysis is limited to the neutron energy loss side due to the experimental setup which was chosen to have its best resolution on the neutron energy loss side. Therefore, transitions on the neutron energy gain side could not be resolved and usefully analyzed.

III. Results and Analysis

Figure 2 shows the low temperature neutron energy loss side spectra of **1**−**3**, taken at 1.8 K (**1** and **3**) and 2.0 K (**2**), respectively. In the spectra of **1** and **2**, two peaks could be observed in each spectrum. In **1** the peaks labeled I_a and I_b are centered at about 10 and 9.3 cm^{-1}, respectively. In **2**, I_c and I_d are observed at about 7.4 and 6.9 cm^{-1}, respectively. The spectrum of **3** shows no resolved peaks in the observed

(8) Boskovic, C.; Brechin, E. K.; Streib, W. E.; Folting, K.; Bollinger, J. C.; Hendrickson, D. N.; Christou, G. *J. Am. Chem. Soc.* **2002**, *124* (4), 3725.
(9) Soler, M.; Artus, P.; Folting, K.; Huffman, J. C.; Hendrickson, D. N.; Christou, G. *Inorg. Chem.* **2001**, *40* (19), 4902.
(10) Brechin, E. K.; Boskovic, C.; Wernsdorfer, W.; Yoo, J.; Yamaguchi, A.; Sanudo, E. C.; Concolino, T. R.; Rheingold, A. L.; Ishimoto, H.; Hendrickson, D. N.; Christou, G. *J. Am. Chem. Soc.* **2002**, *124* (33), 9710.
(11) Andres, H.; Basler, R.; Blake, A. J.; Cadiou, C.; Chaboussant, G.; Graig, M.; Güdel, H. U.; Murrie, M.; Parson, S.; Paulsen, C.; Semadini, F.; Villar, V.; Wernsdorfer, W.; Winpenny, R. E. P. *Chem.*−*Eur. J.* **2002**, *8* (21), 4867.
(12) Ochsenbein, S. T.; Murrie, M.; Rusanov, E.; Stöckli-Evans, H.; Sekine, C.; Güdel, H. U. *Inorg. Chem.* **2002**, *41* (20), 5133.
(13) Chakov, N. E. et al. In preparation.
(14) Soler, M.; Wernsdorfer, W.; Abboud, K. A.; Huffman, J. C.; Davidson, E. R.; Hendrickson, D. N.; Christou, G. *J. Am. Chem. Soc.* **2003**, *125*, 3576.
(15) Mirebeau, I.; Hennion, M.; Casalta, H.; Andres, H.; Güdel, H.-U.; Irodova, A. V.; Caneschi, A. *Phys. Rev. Lett.* **1999**, *83*, 628.
(16) Hennion, M.; Pardi, L.; Mirebeau, I.; Suard, E.; Sessoli, R.; Caneschi, A. *Phys. Rev. B* **1997**, *56*, 8819.
(17) Chaboussant, G.; Güdel, H.-U.; Honecker, A.; Fukushima, N.; Murrie, M.; Normand, B. In preparation.
(18) Andres, H.; Basler, R.; Güdel, H.-U.; Aromi, G.; Christou, G.; Büttner, H.; Rufflé, B. *J. Am. Chem. Soc.* **2000**, *122* (50), 12469.
(19) Basler, R.; Chaboussant, G.; Cañada-Vilalta, C.; Christou, G.; Mutka, H.; Janssen, S.; Altorfer, F.; Güdel, H.-U. *Polyhedron* **2003**, *22*, 2471.
(20) Carretta, S.; Livotti, E.; Amoretti, G.; Caciuffo, R.; Caneschi, A.; Gatteschi, D. *Phys. Rev. B* **2002**, *65*, 052411.
(21) Amoretti, G.; Caciuffo, R.; Combet, J.; Murani, A.; Caneschi, A. *Phys. Rev. B* **2000**, *62*, 3022.

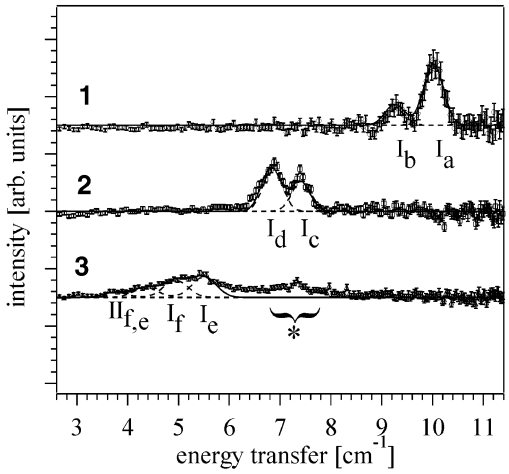

Figure 2. Neutron energy loss side INS spectra of **1** and **3** at $T = 1.8$ K and **2** at $T = 2.0$ K obtained at an incident neutron wavelength $\lambda = 6.0$ Å (NEAT, HMI).

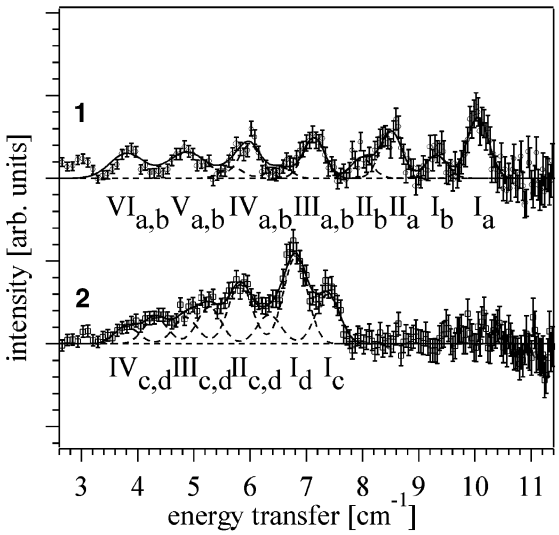

Figure 3. Neutron energy loss side INS spectra of **1** and **2** at $T = 20$ K and $T = 9.9$ K, respectively, obtained at an incident neutron wavelength $\lambda = 6.0$ Å (NEAT, HMI).

energy region, but weak intensity between about 3 and 6 cm^{-1}. The asterisk marks the energy transfer position of an impurity of **2** in **3**. Figure 3 shows spectra of **1** and **2** at 20 and 9.9 K, respectively. For **1**, new transitions, labeled II_a-VI_a and II_b-VI_b, appear at energies between about 3 and 9 cm^{-1} as the temperature is increased. Three new peaks appear in **2** upon raising the temperature to 9.9 K, labeled II_c-IV_c and II_d-IV_d. The solid lines in each spectrum in Figures 2 and 3 correspond to the sum of the Gaussians underlined (dotted lines) in the analysis.

The average energy of transitions I_a and I_b of **1** in Figure 2 is centered at about 9.8 cm^{-1}. Assuming that this corresponds to the first allowed transition between $M_s = \pm 10$ and $M_s = \pm 9$ in the $S = 10$ ground state, its energy is given by $19D$, which means that $D \sim -0.51$ cm^{-1}. Taking this value, the observation of two transitions at 1.8 K for **1** in Figure 1 is puzzling. According to Boltzmann statistics, just the $M_S = \pm 10$ state is populated at 1.8 K (99.9%). Thus, due to the INS selection rule within a given S state, $\Delta M_S = \pm 1$, only one transition should be observed, as is the case for Mn_{12}−acetate.[15] The observation of two peaks in the low temperature spectra of **1** is attributed to two isomers present in the sample, either due to Jahn−Teller isomerism known in Mn_{12} compounds[22,23] or structural isomers.[24,25] Thus, the peaks I_a and I_b correspond to transitions from $M_s = \pm 10$ to $M_s = \pm 9$ energy levels in isomer **a** and isomer **b**, respectively. The ratio **a** to **b** is about 3:1 with the assumption the INS intensities are proportional, within a good accuracy, to the amount of each isomer in the sample.

The same explanation is valid for compound **2**, where the same kind of observations are made. Here, the two peaks labeled I_c and I_d correspond to the isomers **c** and **d** (ratio **c**/**d** = 0.7). A closer look at the data in Figure 2 also reveals the existence of two isomers in **3**, but in this case higher states are already populated at 1.8 K. Thus, hot peaks superimpose with the cold ones and lead to the broad band observed between 3 and 7 cm^{-1}. The two isomers identified are named **e** and **f**. The ratio **e/f** could not be determined from the present data.

On the basis of this information, data are fitted with Gaussians of equal width for each sample, shown as dashed lines in Figures 2 and 3. The width (fwhm) of the Gaussians for the elevated temperature data are fixed to the width of the corresponding transition I at low temperature (about 60 μeV). Exceptions are transitions V_a/V_b and VI_a and VI_b, respectively. For those, it is not possible to locate their four individual positions, because they are superimposed. Thus, V_a/V_b and VI_a/VI_b are treated as one transition for their position with fwhm of about 100 μeV. The results of this procedure are presented in Table 1 for **1**, and the resulting energy splitting patterns for the two isomers **a** and **b** in **1** are shown in Figure 4. In the following analysis, the bands V and VI are not included, due to their overlap problem mentioned above. The experimental energy patterns in Figure 4 are reproduced by applying the following axial Hamiltonian for the magneto-crystalline anisotropy

$$\hat{H} = D\left[\hat{S}_z^2 - \frac{1}{3}S(S+1)\right] + B_4^0\hat{O}_4^0 \qquad (1)$$

where B_4^0 is the axial fourth order term to the zero-field splitting, and $\hat{O}_4^0 = 35\hat{S}_z^4 - [30S(S+1) - 25]\hat{S}_z^2 - 6S(S+1) + 3\hat{S}^2(S+1)^2$. Small deviations from tetragonal symmetry have been neglected in our analysis as they only marginally influence the low energy levels.

Calculations using only the D parameter cannot reproduce the experimental data. Thus, B_4^0 is significant. This allows us to reproduce the deviations of our experimental peak positions from a pure Landé pattern, observed for **1** and **2**. For **3**, the data do not contain enough information to extract the B_4^0 parameter, and thus, this is neglected in the analysis

(22) Aubin, S. M. J.; Sun, Z.; Guzei, I. A.; Rheingold, A. L.; Christou, G.; Hendrickson, D. N. *Chem. Commun.* **1997**, 2239.
(23) Sun, Z.; Ruiz, D.; Rumberger, E.; Incarvito, C. D.; Folting, K.; Rheingold, A. L.; Christou, G.; Hendrickson, D. N. *Inorg. Chem.* **1998**, *37*, 4758.
(24) Cornia, A.; Sessoli, R.; Sorace, L.; Gatteschi, D.; Barra, A. L.; Daiguebonne, C. *Phys. Rev. Lett.* **2002**, *89*, 257201.
(25) Cornia, A.; Fabretti, A.; Sessoli, R.; Sorace, L.; Gatteschi, D.; Barra, A. L.; Daiguebonne, C.; Roisnel, T. *Acta Crystallogr.* **2002**, *58*, 371.

Table 1. Experimental (Neutron Energy Loss Side) and Calculated Energies and Relative Intensities of the INS Transitions of Isomers **a** and **b** In $[Mn_{12}O_{12}(O_2CC_6F_5)_{16}(D_2O)_4]$ (Sample **1**) at $\lambda_i = 6.0$ Å[a]

	isomer **a**							isomer **b**					
	energy [cm^{-1}]		norm int [arb units]					energy [cm^{-1}]		norm int [arb units]			
			2.0 K		20.0 K					2.0 K		20.0 K	
	expt	calcd	expt	calcd	expt	calcd		expt	calcd	expt	calcd	expt	calcd
I_a	10.03(2))	10.01	1.00(3)	1.00	0.37(2)	0.44	I_b	9.30(5)	9.28	1.00(8)	1.00	0.35(2)	0.42
II_a	8.48(2)	8.51			0.29(2)	0.41	II_b	7.90(1)	7.94			0.29(2)	0.41
III_a	7.11(2)	7.16			0.24(2)	0.31	III_b	6.69(2)	6.72			0.24(2)	0.33
IV_a	5.98(3)	5.94			0.19(2)	0.24	IV_b	5.65(1)	5.61			0.18(2)	0.25
V_a	4.86(2)	4.83				0.18	V_b	4.86(2)	4.59				0.20
VI_a	3.79(2)	3.82				0.14	VI_b	3.79(2)	3.65				0.16

[a] The intensities were scaled to a value of 1.0 for transitions I_a and I_b at 2.0 K. For the calculation the following sets of parameters were used: for isomer **a**, $D = -0.463$ cm^{-1} and $B_4^0 = -2.09 \times 10^{-5}$ cm^{-1} with $\chi^2 = 7.7 \times 10^{-4}$; for isomer **b**: $D = -0.437$ cm^{-1} and $B_4^0 = -1.69 \times 10^{-5}$ cm^{-1} with $\chi^2 = 5.4 \times 10^{-4}$.

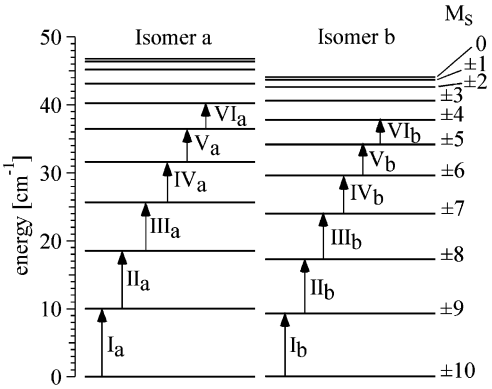

Figure 4. Energy level diagram for **1** calculated using the parameters given in Table 1.

of **3**. Fitting the data with the Hamiltonian (eq 1), the zero-field splitting parameters for the six isomers are determined. They are collected in Table 2.

Using INS, one has information not only on peak positions, but also on their relative intensities. Since the intensity of a given transition is a function of the underlying wave functions of the initial and final states, it is very sensitive to the applied model parameters. Comparing experimental intensities and calculated ones is therefore an excellent way to validate the chosen model.

The differential magnetic neutron cross section for a transition $\Psi_i \rightarrow \Psi_j$ is given by[26]

$$\frac{d^2\sigma}{d\Omega dE} = \frac{N}{4}\left\{\frac{\gamma e^2}{m_e c^2}\right\}^2 \frac{|k'|}{|k|} \exp^{-2W(\mathbf{Q})} F^2(\mathbf{Q}) \times \sum_{\alpha,\beta}\left\{\delta_{\alpha\beta} - \frac{Q_\alpha Q_\beta}{\mathbf{Q}^2}\right\} \times \sum_{i,j} \exp^{i\vec{\mathbf{Q}}(\vec{\mathbf{R}}_i - \vec{\mathbf{R}}_j)} \langle\Psi_i|\hat{S}_i^\alpha|\Psi_j\rangle \times \langle\Psi_j|\hat{S}_j^\beta|\Psi_i\rangle \delta(\hbar\omega + E_j - E_i) \quad (2)$$

In this equation, k and k' are the wavenumbers of the incoming and scattered neutrons, **Q** is the scattering vector, $\exp(-2W)$ is the Debye−Waller factor, $\hbar\omega$ is the neutron energy, and Ψ_i and Ψ_j are the cluster wave functions with energies E_i and E_j, respectively. g_i is the g factor, and $F(\mathbf{Q})$ is the magnetic form factor. $\vec{R}_i$ is the space vector of the ith Mn ion in the cluster, and α and β stand for the spatial coordinates x, y, and z. e and m_e are the charge and mass of the electron, respectively, c is the speed of light, and $\gamma = -1.91$ is the gyromagnetic constant of the neutron.

Table 2. Zero-Field Splitting Parameters D and B_4^0 (in cm^{-1}) in the Three Samples

	isomers					
param [cm^{-1}]	**1a**	**1b**	**2c**	**2d**	**3e**	**3f**
D	−0.463	−0.437	−0.368	−0.332	−0.274	−0.241
$B_4^0[10^{-5}]$	−2.09	−1.69	−1.59	−1.80		
$\chi^2[10^{-3}]$	0.8	0.5	0.4	3.8	4	7

For a powder sample, eq 2 has to be averaged in Q-space. For the relative intensities we are then left with[27]

$$\frac{d^2\sigma}{d\Omega dE} \sim \sum_{i,f} p_i |\langle\Psi_i| S_\perp |\Psi_j\rangle|^2 \quad (3)$$

$S_\perp$ is the spin component perpendicular to the scattering vector **Q**, and p_i is the Boltzmann factor of level i. The results of these calculations are given in Table 1 for both isomers of compound **1**. The overall agreement with the experimental data is very good.

IV. Discussion

The $S = 10$ ground state of the neutral compounds is empirically understood by considering the ferrimagnetic arrangement first suggested for Mn_{12}−acetate (see Introduction). As one Mn^{3+} is reduced to a Mn^{2+}, one would intuitively expect a spin ground state $S = {}^{21}/_2$ instead of $S = {}^{19}/_2$. With one more electron reduction step, we recover $S = 10$ again, but we would naively expect $S = 11$. This pattern clearly shows that the canonical picture of the Mn_{12} ground state should be handled with great care, as it can easily predict the wrong ground state. This is due to several factors: The ground state is extremely dependent on the competition between the various exchange couplings in the cluster and any change like swapping one Mn^{3+} for one Mn^{2+} can considerably modify the low energy levels. We know

(26) Marshall, W.; Lovesey, S. W. *Theory of Thermal Neutron Scattering*; Clarendon Press: Oxford, 1971.

(27) Birgenau, R. J. *J. Phys. Chem. Solids* **1972**, *33*, 59.

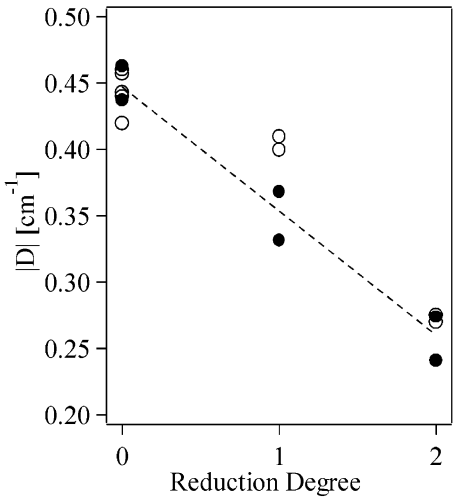

Figure 5. Dependence of the zero-field splitting parameter *D* as a function of the degree of reduction. The dashed line is drawn to aid in visualization. The parameters were taken from refs 15, 30, 28, 29, 14 (○) and the present data (●).

that in Mn_{12}−acetate low energy spin states are lying not far from the ground state, the first one as low as 40 cm^{-1},[16,17] and a few percent change in the exchange couplings can alter the energy level ordering.

The anisotropy parameter *D* decreases as our Mn_{12} complexes get successively reduced, see Table 2 and Figure 5. The *D* values given in Table 2 are approximate values because the fitting model assumes axial symmetry, and these complexes are all crystallographically occupying nonaxial sites.[13] The decrease in *D* of about 25% upon each reduction step is also observed in other Mn_{12} analogues.[14,15,29−30] A comparison between reported *D* values and the present data is shown in Figure 5. Upon one-electron reduction step, the added electron is preferably located on a ring Mn atom. This process is asserted by Mn−O bond length calculations, and the oxidation levels were estimated by bond valence sum (BVS) calculations.[13] The decrease of the cluster anisotropy can thus be explained by the decreasing number of Mn^{3+} ions from eight in sample **1** to six in sample **3**. Removing a Mn^{3+} ion results in the loss of one Jahn−Teller axis in the ring.

The cluster anisotropy parameter *D* essentially derives from the single-ion anisotropy parameter D_i of the individual Mn^{3+} ions. The single-ion anisotropy of the Mn^{2+} and Mn^{4+} are assumed to be negligible compared to the strongly Jahn−Teller distorted Mn^{3+} ions. The exact relationship between *D* and D_i is possible if the exact spin combination giving the ground state is known.[31] For Mn_{12}−acetate, the ground state configuration is relatively well established, and assuming that D_i is zero for the Mn^{4+} ions and D_i is equal for all Mn^{3+} ions, we get $D \sim 0.23D_i$ and thus $D_i \sim 2$ cm^{-1} for **1**. The situation is less straightforward for the electron reduced compounds because they have different ground states.

We see that the added electron reduction leads to a decrease of the axial anisotropy parameter *D*, but it is apparent that the anisotropy reduction of the ground state is more important than anticipated assuming a linear relationship between the number of Mn^{3+} ions present in the cluster and the parameter *D*. In other words, the loss of one (or two) JT distorted sites not only quenches the single-ion anisotropy on these sites but affects the whole cluster anisotropy in a collective way.

Finally, the $S = 10$ value of the $[Mn_{12}]^{2-}$ complexes, together with an anisotropy that has been decreased but is still reasonably large, explains why they still function as SMMs at low temperatures, i.e., still possess a sufficiently large barrier to magnetization reversal to display slow magnetization relaxation rates. The upper limit for the energy barrier ΔE can be evaluated for the three compounds as the following: $\Delta E = -S^2D = 45$ cm^{-1} for $z = 0$, $\Delta E = -(S^2 - {}^1/_4)D = 31$ cm^{-1} for $z = -1$, and $\Delta E = 26$ cm^{-1} for $z = -2$.

V. Conclusion

Using INS spectroscopy, we have clearly shown the effect of electron reduction in Mn_{12} derivatives. The spin ground state varies from $S = 10$ for the neutral and two-electron reduced compounds to $S = {}^{19}/_2$ for the one-electron reduced species. This result is somewhat counterintuitive but stems from the fact that the ground state is the result of multiple competitive exchange interactions within the cluster.[17,32] Only the knowledge of all the exchange couplings will permit a definitive rationalization of the ground state evolution as a function of electron reduction. On the other hand, the anisotropy is clearly reduced upon adding electrons. The extra electron preferably reduces a Mn^{3+}, hence converting them to magnetically almost isotropic Mn^{2+}. We find an almost linear relationship between the degree of electron reduction and the axial anisotropy parameter of the cluster. Further theoretical work is needed in order to completely understand the effect of additional electrons in such single molecule magnets.

Acknowledgment. This work has been supported by the Swiss National Science Foundation, the TMR Program Molnanomag of the European Union (HPRN-CT-1999-00012), and the United States National Science Foundation.

IC048931P

(28) Soler, M.; Artus, P.; Folting, K.; Huffman, J. C.; Hendrickson, D. N.; Christou, G. *Inorg. Chem.* **2001**, *40*, 4902.
(29) Aubin, S. M. J.; Sun, Z.; Pardi, L.; Krzystek, J.; Folting, K.; Brunel, L. C.; Rheingold, A. L.; Christou, G.; Hendrickson, D. N. *Inorg. Chem.* **1999**, *38*, 5329.
(30) Eppley, H. J.; Tsai, H.; deVries, N.; Folting, K.; Christou, G.; Hendrickson, D. N. *J. Am. Chem. Soc.* **1995**, *117* (1), 301.
(31) Andres, H.; Clemente-Juan, J. M.; Basler, R.; Aebersold, M.; Güdel, H.-U.; Borras-Almenar, J. J.; Gaita, A.; Coronado, E.; Büttner, H.; Janssen, S. *Inorg. Chem.* **2001**, *40* (8), 1943.
(32) Regnault, N.; Jolicoeur, T.; Sessoli, R.; Gatteschi, D.; Verdaguer, M. *Phys. Rev. B* **2002**, *66*, 054409.